Elastic magnetic form factor of ^{6}Li

J. C. Bergstrom
Saskatchewan Accelerator Laboratory, University of Saskatchewan, Saskatoon, Canada S7N OWO

S. B. Kowalski
Bates Accelerator Center, Laboratory for Nuclear Science and Department of Physics, Massachusetts Institute of Technology, Cambridge, Massachusetts 02139

R. Neuhausen
Institut für Kernphysik der Universität Mainz, 6500 Mainz, Germany

(Received 2 November 1981)

The magnetic form factor for the ground state of ^{6}Li has been measured for momentum transfers $q=0.8-2.8$ fm^{-1}. The diffraction minimum has been located at $q=1.41$ fm^{-1}, and the results extend over the second maximum. All available longitudinal and transverse form factors of ^{6}Li are shown to be consistent with the α-d cluster model providing the d cluster is deformed and aligned. Comparison is made between the elastic and 3.56 MeV $M1$ form factors, and the effects of exchange currents are considered. The ground-state current density is deduced by a Fourier-Bessel analysis of the elastic $M1$ data.

[NUCLEAR REACTIONS ^{6}Li(e,e'), $E=80-300$ MeV; $\sigma(E;E_{e'},\theta)$. ^{6}Li deduced elastic $M1$ form factor. Cluster model. Exchange currents. Current density.]

I. INTRODUCTION

Excluding the few broad resonances above 20 MeV excitation, ^{6}Li has only five known excited states, all below 6 MeV. With one exception, all are clearly seen in electron scattering and most of the corresponding form factors have been measured over a wide range of momentum transfers. The exception is the 5.65 MeV $(1^+,T=0)$ level. It is not clear why this level has not been seen unless its natural width is very large, i.e., greater than 2 MeV, in which case it would be hidden by the rather broad peaks from the 4.31 MeV $(2^+,T=0)$ and 5.37 MeV $(2^+,T=1)$ excitations. The 4.31 MeV transition is quite evident but its form factor has not been determined because of the large natural width ($\Gamma\sim 1$ MeV), the proximity of other levels, and the strong underlying continua.

Aside from these two cases, only the elastic magnetic form factor remained relatively unknown. Some indication of the q dependence comes from the Amsterdam[1] and Stanford[2] work; however, the former are confined to $q<0.9$ fm^{-1}, while the latter extend to 1.4 fm^{-1} but with poor statistics.

In this paper we present new measurements of the elastic magnetic form factor for momentum transfers $q=0.8-2.8$ fm^{-1}. The location of a diffraction minimum has been clearly established at $q=1.41\pm 0.03$ fm^{-1}, and the data extend over the second maximum of the form factor. The statistical accuracy of this work is considerably improved over the previous measurements where they overlap.

Since ^{4}He is a strongly bound system, it has been assumed that the low-lying features of ^{6}Li can be treated to first order as a three-body problem consisting of an inert α core plus two relatively weakly bound nucleons. Support for this picture comes from three-body calculations of $A=6$ nuclei using realistic N-N and N-α interactions, and although these have focused on the ground states, the results are encouraging.[3]

Electron scattering can provide a good test for such calculations since it is sensitive to the spatial dependence of the charge and current densities. However, to date there have been very few estimates made of the electromagnetic form factors of ^{6}Li in the three-body model. The ground state is a logical starting point for comparing theory and experiment, but the charge form factor does not in itself provide a sufficient test since the dynamical aspects as

represented by the current density must also be considered. The latter contributes to the magnetic form factor, and hence provides one motivation for the present experiment. Hopefully, the availability of both form factors will encourage further theoretical development in this direction.

The elastic form factors place strong constraints on the various phenomenological descriptions such as the two-body cluster models. These macroscopic models are useful in that they often provide simple interpretations of phenomena that are rather complex at the microscopic level. In view of the apparent failure of the cluster models to give a reasonable account of the elastic Coulomb and inelastic (3.56 MeV) magnetic form factors within a common basis,[4] it becomes important to see how the models compare with both elastic form factors.

Finally, it is well known that two-body processes such as meson exchange currents make negligible contributions to the ground state $M1$ scattering due to its isoscalar nature, but they can affect the isovector $M1$ transition to the 3.56 MeV $(0^+, T=1)$ state. By comparing these form factors some insight might be gained as to the order of magnitude of the two-body effects in ^{6}Li.

The present paper is organized as follows. First, the experimental details and data analysis are discussed, with particular attention to the Coulomb correction near 180°, and the experimental results are given. In Sec. III we show that all the known form factors below 6 MeV excitation can be described by a simple α-d cluster model providing the "deuteron" cluster is deformed and aligned. In Sec. IV the elastic $M1$ and inelastic (3.56 MeV) $M1$ form factors are compared and the influence of exchange currents is considered. Finally, in Sec. V we give the ground state current density based on a Fourier-Bessel analysis of the magnetic form factor.

II. EXPERIMENTAL DETAILS AND DATA ANALYSIS

This experiment was performed at the electron scattering facility of the MIT-Bates accelerator laboratory.[5] Scattering angles varied between 150° and 180°, and for the latter the four-magnet 180° scattering system was utilized.[6] The dispersed-beam mode was used at all angles so currents up to 30 μA could be endured by the lithium targets, although as a precaution most runs were made at $\sim$20 μA.

The ^{6}Li targets were rolled from 98.7% isotopically enriched metal and varied in thicknesses from 26.20 to 94.79 mg/cm^2. The main impurity, ^{7}Li, gives an inelastic peak from the 0.478 MeV level which at certain energies cannot be resolved from the ^{6}Li elastic peak due to the differential recoil of the nuclei. To correct for this, data were also obtained with ^{7}Li targets enriched to 99.9% and of thicknesses similar to the ^{6}Li targets. The energy calibration of the incident beam was determined from the differential recoil of the ^{7}Li 4.633 MeV peak relative to the 2.185 and 3.562 MeV peaks from ^{6}Li.

For the most part, the data were normalized using the known system parameters. The overall efficiency was checked periodically against the proton by scattering from a 23.6 mg/cm^2 rotating polyethylene target. Cross checks were also made whenever possible against the 3.56 MeV $M1$ form factor of ^{6}Li (Ref. 7). Consistency with the system calibration was always achieved above 140 MeV, but at lower energies both checks showed a monotonically-decreasing detector efficiency, subsequently traced to the Cerenkov counters. Therefore, below 140 MeV we have relied on the experimental efficiencies and included their uncertainties in the final data errors.

The raw data were converted to cross sections in the usual way by integrating the elastic peaks out to some cutoff energy ΔE and then by applying various factors to correct for radiative and straggling phenomena. Although the straggling factors were essentially unity, the radiative corrections were as large as 1.4. We have used a version of the radiative correction in which the soft-photon term is exponentiated as discussed by Maximon.[8] Checks were made to ensure that the cross sections were independent of ΔE within statistics, and the reliability of the corrections were verified occasionally by normalizing the elastic peak to the 3.56 MeV form factor.

The magnetic moment of ^{6}Li is small and therefore the charge scattering is predominant at all but the largest scattering angles. In practice, even the 180° measurements contain a sizable Coulomb contribution for energies below $\sim$200 MeV. At higher energies the Coulomb form factor rapidly decreases, allowing measurements to be made at scattering angles of 150°$-$160°, where the targets could be oriented in the so-called transmission mode to achieve optimum resolution and counting rates.

The finite angular acceptance of the spectrometer and multiple scattering in the targets enhance the Coulomb effects near 180°. Since our estimate of the multiple scattering differs from previous treatments,[9] we will review the basic equations.

The probability that an electron will enter the target and multiply scatter down to a depth t, undergo a near-180° deflection by the nuclear Coulomb field in a layer dt, and then multiply scatter back to emerge into a solid angle $d\Omega$ at a small angle ϵ to the true 180° direction, is

$$P(t,dt)=\tfrac{1}{4}\sigma_0 F_C{}^2\left[\epsilon^2+2\langle\theta^2\rangle_t+\frac{4}{\gamma^2}\right]N\,d\Omega\,dt\ . \quad (1)$$

Here, F_C is the Coulomb form factor, γ is the ratio of the electron energy to its rest energy, N is the number of nuclei per unit volume, and

$$\sigma_0=\frac{1}{\eta}\left[\frac{Ze^2}{2E_0}\right]^2,$$

$$\eta=1+\left[\frac{2E_0}{M}\right]\sin^2\left[\frac{\pi-\epsilon}{2}\right], \quad (2)$$

where the symbols in Eq. (2) have their usual meaning. Finally, $\langle\theta^2\rangle_t$ is the mean-square multiple scattering angle after traversing a thickness t of material. In deriving Eq. (1) we have assumed the total path length does not deviate appreciably from $2t$.

Equation (1) is essentially equivalent to a derivation by Rand[9] [Eq. (6)]. However, we go further and integrate Eq. (1) over the target thickness to obtain the effective Coulomb differential cross section

$$\left[\frac{d\sigma_C}{d\Omega}\right]_{\text{eff}}=\tfrac{1}{4}\sigma_0 F_C{}^2\left[\epsilon^2+2\langle\theta^2\rangle+\frac{4}{\gamma^2}\right], \quad (3)$$

where

$$\langle\theta^2\rangle=\frac{1}{t_0}\int_0^{t_0}\langle\theta^2\rangle_t dt \quad (4)$$

and t_0 is the target thickness.

The multiple scattering is evaluated using the Molière theory as reviewed by Bethe and Ashkin,[10] retaining only the leading Gaussian term. Thus,

$$\langle\theta^2\rangle_t=0.157Z\left[\frac{Z+1}{A}\right]\left[\frac{t}{E_0{}^2}\right]B\ , \quad (5)$$

where t is in g/cm^2 and E_0 is in MeV. The parameter B is the solution to a transcendental equation but can be approximated by

$$B\approx\alpha+\beta\ln[7800Z^{1/3}(Z+1)t/A]\ . \quad (6)$$

With the help of Table IX in Ref. 10 and related equations, we find $\alpha\approx1.01$ and $\beta\approx1.15$ for the present targets. (For comparison, the equivalent constants used by Rand are $\alpha=1.5$, $\beta=1.1$.) The integral in Eq. (4) may now be done in closed form and one obtains

$$\langle\theta^2\rangle=\langle\theta^2\rangle_{t_0}\left[\frac{1}{2}-\frac{\beta}{4B}\right]$$

$$\approx\tfrac{1}{2}\langle\theta^2\rangle_{t_0}\text{ since }B\approx7-9\ . \quad (7)$$

Finally, Eq. (3) must be integrated over the spectrometer acceptance angles, θ_h and θ_v in the horizontal and vertical planes, respectively. If the magnetic scattering is also included, the total experimental cross section near 180° may be written

$$\sigma_{\text{tot}}\approx\sigma_0\left[F_M{}^2+F_C{}^2\left[\frac{\theta_h{}^2+\theta_v{}^2}{48}+\frac{\langle\theta^2\rangle_{t_0}}{4}+\frac{1}{\gamma^2}+\frac{\epsilon_0{}^2}{4}\right]\right]\Delta\Omega\ , \quad (8)$$

where $\Delta\Omega=\theta_h\theta_v$ and $\pi-\epsilon_0=\theta$ is the nominal scattering angle as prescribed by the spectrometer and deflecting magnets. Our definition of the magnetic form factor F_M is similar to that used in inelastic scattering, being related to the magnetic cross section by

$$\frac{d\sigma_M}{d\Omega}=\sigma_0\frac{\cos^2\frac{1}{2}\theta}{\sin^4\frac{1}{2}\theta}(\tfrac{1}{2}+\tan^2\tfrac{1}{2}\theta)F_M{}^2\ . \quad (9)$$

An experimental check of the Coulomb correction was made at 80 MeV for a range of spectrometer apertures ($\Delta\Omega=0.7-2.8$ msr) and two ^{6}Li targets (26 and 95 mg/cm^2). The Coulomb terms were evaluated according to Eq. (8) with $\sigma_0F_C{}^2$ as computed by a phase-shift code using the charge distribution from Ref. 11. After correcting the data for charge scattering, up to 50% in some cases, the remaining magnetic cross sections were found to be self-consistent within statistical errors.

Under ideal conditions $\epsilon_0=0$, but since the alignment of the 180° system had not been optimized for very light nuclei, we have included an uncertainty of 0.5° in ϵ_0 and propagated this to our final errors. This contribution is insignificant for energies $E_0>140$ MeV.

The final experimental results are summarized in Table I and are plotted as the black points in Fig. 1. For comparison, we have also included the Amsterdam data,[1] shown as the open circles, and the agreement between the two data sets is seen to be quite good.

The present analysis was done in the Born ap-

TABLE I. Tabulation of the elastic $M1$ form factor of ^{6}Li as determined by the present experiment.

E_0 (MeV)	θ (deg)	q (fm^{-1})	$F_{M1}{}^2$ ($\times 10^{-6}$)
80.0	180°	0.80	91.5 ±5.6
100.0	180°	1.00	32.5 ±3.4
120.0	180°	1.19	6.7 ±1.5
140.0	180°	1.39	<0.5
160.0	180°	1.58	3.4 ±1.0
179.6	180°	1.76	5.00±0.51
195.5	180°	1.92	7.10±0.54
215.5	180°	2.11	6.56±0.50
230.3	180°	2.24	5.10±0.44
257.1	150°	2.42	3.06±0.37
255.8	160°	2.45	3.51±0.38
267.1	150°	2.51	2.38±0.26
282.4	150°	2.64	1.76±0.17
283.0	150°	2.65	1.82±0.18
297.8	150°	2.78	1.17±0.11

proximation [i.e., Eq. (9)] and no corrections were made for Coulomb distortion. One can partially take this into account by using the effective momentum transfer q_{eff}, given by

$$q_{\text{eff}} = q\left[1+\frac{3\alpha Z}{2E_0 R}\right], \tag{10}$$

where $R=(\frac{5}{3})^{1/2}r_{\text{rms}}$ is the radius of the equivalent sphere.

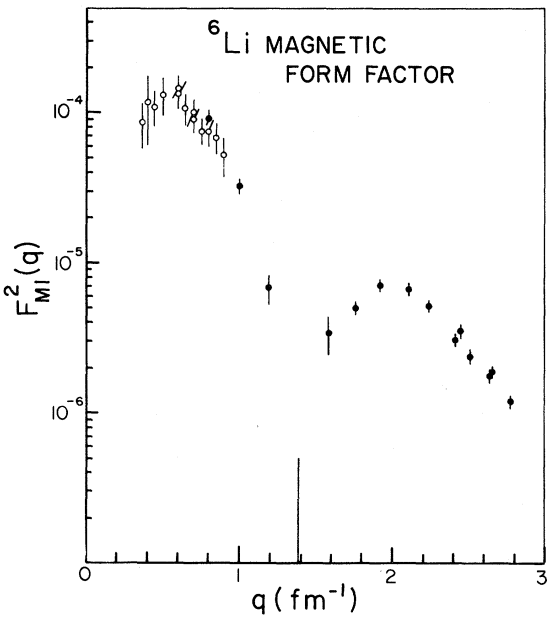

FIG. 1. The elastic $M1$ form factor of ^{6}Li as determined by the present work (black points), and the Amsterdam results (open circles). No corrections have been made for Coulomb distortion. Our definition of the magnetic form factor is similar to that used in inelastic scattering [Eq. (9)].

III. PHENOMENOLOGICAL α-d CLUSTER MODEL

A. Formalism and comparison with experiment

The α-d cluster model has been used for several years as a basis for describing the low-lying structure of ^{6}Li, with varying degrees of success. The phenomenological version pioneered by Kudeyarov *et al.*[12] was among the first antisymmetrized cluster models to be applied to the electromagnetic form factors, and showed the vital role played by antisymmetrization, particularly for the transverse form factors. In this version there are only three parameters; the internal alpha-particle oscillator parameter α, the internal deuteron parameter β, and γ representing the relative motion of the clusters. The usual $(1s)^4(1p)^2$ harmonic oscillator shell model obtains in the limit $\gamma=\beta=\alpha$.

A more recent study[4] concluded that the longitudinal form factors of the ground and first excited states of ^{6}Li can be understood within the context of the phenomenological α-d model, but not the transverse form factors of other levels. In particular, the 3.56 MeV $M1$ diffraction minimum occurs at a somewhat higher momentum transfer ($q=1.4$ fm^{-1}) than predicted, and no reasonable choice for

β or γ improves the situation. A similar problem occurs with the ground state magnetic form factor, which also has a minimum near $q=1.4$ fm^{-1}. Oddly enough, both $M1$ form factors are more consistent with a t-τ cluster model, but the corresponding elastic Coulomb form factor disagrees markedly with experiment.

It is our purpose here to show that a consistent description of *all* the available form factors of ^{6}Li can be achieved within the framework of the phenomenological α-d model if we permit the deuteron cluster to deform, or stretch, along a line connecting the cluster centers of mass. Actually, this apparent *ad hoc* modification has a simple interpretation in the familiar shell model, as will be seen shortly.

As usual, we use L-S coupling and retain only the dominant configuration of each state; $^3S_1$ for the ground state, $^1S_0$ for the 3.56 MeV level, etc.[4] The wave function for a state with angular momentum J and isospin T is given by

$$\Psi_{JT}=\hat{A}[(\psi_\alpha\otimes\psi_d)_{ST}\otimes\phi_L(\vec{\mathrm{R}})]_{JT}\ , \tag{11}$$

where $\hat{A}$ is the antisymmetrization operator, and

$$\psi_\alpha=\exp\left[-\tfrac{1}{2}\alpha\sum_{i=1}^{4}(\vec{\mathrm{r}}_i-\vec{\mathrm{R}}_\alpha)^2\right]\chi_\alpha\ , \tag{12}$$

$$\psi_d=\exp\left[-\tfrac{1}{2}\beta\sum_{i=5}^{6}(\vec{\mathrm{r}}_i-\vec{\mathrm{R}}_d)^2 -\tfrac{3}{4}\Delta\beta(r_6^2-r_5^2)\right]\Bigg|_{\mathrm{sym}}\chi_d\ , \tag{13}$$

$$\phi_L(\vec{\mathrm{R}})=R^2Y_{LM}(\Omega_R)\exp(-\tfrac{2}{3}\gamma R^2)\ . \tag{14}$$

Here, $\vec{\mathrm{R}}=\vec{\mathrm{R}}_d-\vec{\mathrm{R}}_\alpha$ is the relative position of the clusters, $\phi_L(\vec{\mathrm{R}})$ is the relative motion function, and $\Delta\beta$ is a measure of the deuteron deformation. The subscript "sym" implies explicit symmetrization of ψ_d with respect to the particles 5 and 6, necessary to preserve the proper spin-isospin symmetries. The appropriate spin-isospin functions are represented by χ; the d cluster is in a triplet and singlet spin state for the $T=0$ and $T=1$ levels, respectively. Finally, we explicitly apply the center of mass constraint $\sum_{i=1}^{6}\vec{\mathrm{r}}_i=0$.

The significance of $\Delta\beta$ can be seen more clearly by writing the d-cluster wave function as

$$\psi_d=e^{(-1/4)\beta r^2}(e^{-\Delta\beta\vec{\mathrm{r}}\cdot\vec{\mathrm{R}}}+e^{\Delta\beta\vec{\mathrm{r}}\cdot\vec{\mathrm{R}}})\chi_d\ , \tag{15}$$

where $\vec{\mathrm{r}}$ is the relative position of the two nucleons. Thus, the $\Delta\beta$ term elongates the cluster along the direction of $\vec{\mathrm{R}}$, the asymmetry increasing with R but weighted by $\phi_L(\vec{\mathrm{R}})$ through Eq. (11). Of course, the actual nucleon distribution will be altered somewhat by the antisymmetrization of Eq. (11), which among other things generates a node in the relative motion function.[12]

It is instructive to express the wave function given by Eqs. (11)–(14) in an alternative form. With the help of the center of mass constraint, we have

$$\Psi_{JT}=\prod_{i=1}^{4}e^{(-1/2)\alpha r_i^2}\left[\prod_{i=5}^{6}e^{(-1/2)b_i r_i^2}\right]_{\mathrm{sym}}e^{(-1/2)c(\vec{\mathrm{r}}_5-\vec{\mathrm{r}}_6)^2}R^2Y_{LM}(\Omega_R)\ , \tag{16}$$

where

$$b_5=\tfrac{1}{2}(3\gamma-\alpha+3\Delta\beta)\ ,$$

$$b_6=\tfrac{1}{2}(3\gamma-\alpha-3\Delta\beta)\ ,$$

$$c=\tfrac{1}{4}(\alpha-3\gamma+2\beta)\ ,$$

and for clarity the spin-isospin functions, antisymmetrization, etc., have been suppressed. Antisymmetrization of the above generates the correct binomial combinations of $\vec{\mathrm{r}}_i$ and $\vec{\mathrm{r}}_j$ from $R^2Y_{LM}(\Omega_R)$, consistent with the Pauli principle and the orbital angular momentum.

According to Eq. (16), the deformed α-d model may be interpreted in a shell model basis as a closed $1s$ core plus two $1p$ valence nucleons whose oscillator parameters b_i differ by $3\Delta\beta$, and which mutually interact through an effective harmonic potential with oscillator parameter c. This "residual" two-body interaction is independent of $\Delta\beta$ and vanishes in the independent-particle shell model limit $\alpha=\beta=\gamma$.

The electromagnetic form factors were calculated with the modified α-d wave functions using the same techniques as in Ref. 4, except here the 2.18 MeV $(3^+,T=0)$ wave function is fully antisymmetrized. Specifically, the levels and multipolarities we have considered are the ground state ($C0$,$M1$), 2.18 MeV ($C2$), 3.56 MeV ($M1$), and 5.37 MeV ($M1+E2+M3$). As before, the proton form factor was explicitly included, and the value of α was determined from the free ^{4}He radius. The

remaining variables $(\beta,\Delta\beta,\gamma)$ were constrained by the ^{6}Li charge radius and the general features of the *elastic* form factors, such as the position of the $M1$ diffraction minimum. The location of this minimum is very sensitive to $\Delta\beta$ and tightly restricts its range of values.

The optimized parameters are

$$\alpha=0.582\ \text{fm}^{-2},\quad \beta/\alpha=0.50\ ,$$
$$\gamma/\alpha=0.41,\quad \Delta\beta/\alpha=0.17\ , \tag{17}$$

and the corresponding form factors are compared with experiment in Fig. 2. For the most part, the model gives a reasonable account of all the data. We now comment briefly on each of the form factors.

1. Ground state (1^+, $T=0$)

The $M1$ form factor [Fig. 2(a)] compares well with the data over the whole range of momentum transfers, but the $C0$ form factor [Fig. 2(b)] shows some disagreement at large q. This may in part be due to the harmonic oscillator representation of the α core which we know does not give a proper description of the ^{4}He Coulomb form factor in the same region. On the other hand, since the magnetic structure is determined by the valence nucleons, the transverse form factors are somewhat less sensitive to the specific core model.

The measured rms radius of ^{6}Li is 2.56 ± 0.05 fm (Ref. 11) compared with 2.50 fm for the present model. The rms radius of the d-cluster function [i.e., Eq. (15)], after integrating over R and including the proton radius, is about 2.1 fm, which (coincidentally) is the same as the free deuteron.

The undeformed α-d model[4] predicts a t-τ spectroscopic factor for the ground state $\theta_0^2(t)=0.41$, while the deformed model gives $\theta_0^2(t)=0.49$, compared with the "experimental" range of values $\theta_0^2(t)=0.6-0.8$.

2. 2.18 MeV state (3^+, $T=0$)

The $C2$ form factor is much too small if the excited-state γ parameter (γ') is equal to the ground-state value, so γ' was optimized to minimize the difference near the top of the form factor, with the result

$$\gamma'/\alpha=0.30\ .$$

That this is smaller than the ground-state quantity is hardly surprising; it reflects the increase in the

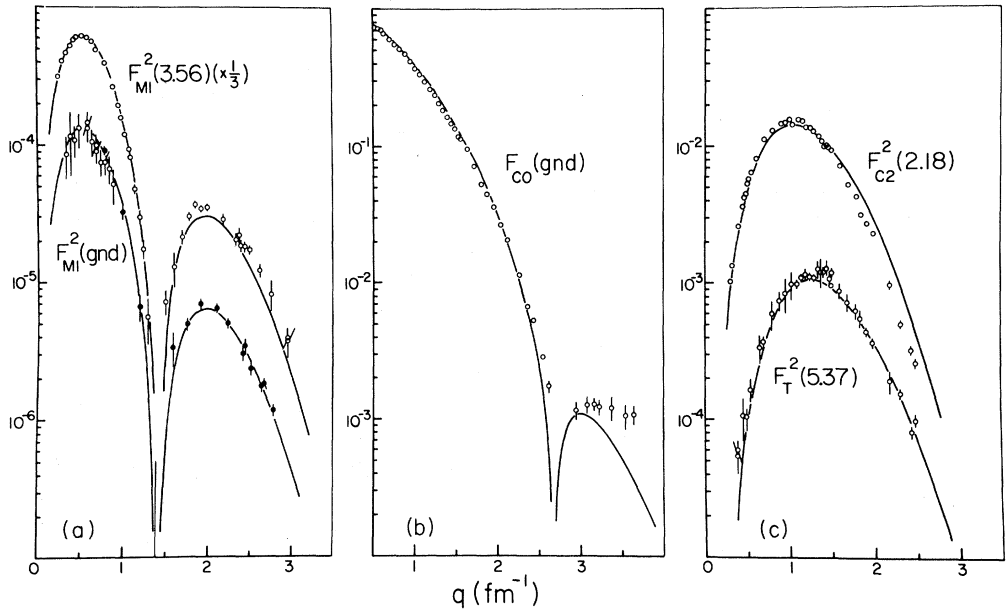

FIG. 2. The known form factors of ^{6}Li compared with the deformed α-d cluster model. The black data points for F_{M1}^2(gnd) are from the present experiment while the open circles are the Amsterdam results (Ref. 1). The F_{M1}^2(3.56) points are from Saskatoon and Mainz (Ref. 7), while the elastic Coulomb data, F_{C0}(gnd), are from Stanford (Ref. 11). The F_{C2}^2(2.18) results are a combination from Darmstadt, Saskatoon, and Mainz (references cited in Ref. 4). The data for F_T^2(5.37) are from five experiments, cited in Ref. 14.

average intercluster separation due to the unbound character (to $\alpha+d$ breakup) of the excited state. The form factor is shown in Fig. 2(c).

The radiative width $\Gamma_{\gamma 0}$ is in better agreement with experiment than the undeformed calculation. The present model gives

$$\Gamma_{\gamma 0}(\alpha-d)=4.0\times 10^{-4}\ \text{eV}\ ,$$

while the experimental value is[13]

$$\Gamma_{\gamma 0}(\text{expt.})=(4.4\pm 0.3)\times 10^{-4}\ \text{eV}\ .$$

3. 3.56 MeV state $(0^+,T=1)$.

The predicted $M1$ form factor, shown in Fig. 2(a), is in very good agreement with the data on the first lobe, and gradually falls away from the data beyond the diffraction minimum. This agreement is particularly noteworthy since we have employed a combination of oscillatorlike functions, while all previous efforts to accurately describe the data on the first maximum have relied on a Woods-Saxon potential in a shell model basis.

Another interesting feature concerns the ratio of the elastic and inelastic $M1$ form factors. One may show on general grounds that the isoscalar and isovector form factors for the transitions ${}^3S_1(T=0)\rightarrow{}^3S_1(T=0)$ and ${}^3S_1(T=0)\rightarrow{}^1S_0$ $(T=1)$ are related by

$$\frac{F_{M1}{}^2(\Delta T=0)}{F_{M1}{}^2(\Delta T=1)}=2\left[\frac{\mu_p+\mu_n}{\mu_p-\mu_n}\right]^2 , \tag{18}$$

where $\mu_{p,n}$ are the nucleon magnetic moments. This relation assumes no change in the radial functions between the ground and excited states. Since the curves in Fig. 2(a) satisfy Eq. (18), it is apparent that the experimental results seem to follow the same trend, except at the higher momentum transfers, even to the extent of having coincident diffraction minima.

The 3.56 MeV level has a P-state component whose amplitude may be as large as 0.5, so it may seem surprising that a model based on a simple spin-flip transition should work so well. As it happens, more complete wave functions such as those derived from electron scattering show that over 90% of the transition amplitude is spin flip in origin. Furthermore, the $M1$ form factor for these wave functions is similar to that calculated in the L-S limit ${}^3S_1\rightarrow{}^1S_0$, and the respective radiative widths differ by less than 2%. Thus, the agreement achieved with the α-d model is probably representative of what could be expected if the cluster basis were expanded to include other L-S configurations.

4. 5.37 MeV state $(2^+,T=1)$.

The transverse form factor for this level is of mixed multipolarity, $M1+E2+M3$. The general wave function in L-S coupling and a $(1p)^2$ configuration space is of the form

$$\Psi_{2^+,1}=G\,{}^3P_2+H\,{}^1D_2\ ,$$

where $G\approx 0.46$ and $H\approx 0.89$ (Ref. 14). However, it may be shown that the D state rapidly dominates the total transverse form factor when $q>0.6$ fm^{-1}, so the cluster model (which contains only the D state) should be valid at higher momentum transfers providing the corresponding form factor (squared) is renormalized by H^2. An additional factor of 1/1.42 is required for technical reasons related to the analysis of the electron scattering spectra.[4]

As seen in Fig. 2(c), we obtain very good agreement with experiment except perhaps at the lowest momentum transfers, where the P-state contribution is not negligible.

B. Discussion

The ground state magnetic form factor provides a strong constraint on the α-d cluster model of ^{6}Li, and only by deforming and aligning the deuteron cluster can we get an acceptable description of both the longitudinal and transverse elastic form factors. The deformed α-d model also yields form factors for the 2.18, 3.56, and 5.37 MeV levels that are in much better agreement with experiment than the usual α-d or t-τ models.

While the cluster model is a convenient way of visualizing the system, it is simply a reflection of structural details originating at a more microscopic level. Thus, from the shell model point of view, Eqs. (16) and (17) show that the two valence nucleons have dissimilar oscillator parameters b_i, and that there is a substantial n-p interaction ($c=0.11$ fm^{-2}), the latter probably reflecting the expected two-body residual interaction. While it is possible to get a good fit to the elastic $M1$ data in the $c=0$ limit, the corresponding Coulomb form factor compares poorly with experiment, even when the rms radius is constrained to the known value. Apparently in ^{6}Li the two-body interaction cannot be completely represented by a suitable one-body central potential, a conclusion also reached in a recent

work by Payne and Nigam.[15] These authors evaluated the relative n-p wave function for specific two-body potentials, and found that a residual Gaussian interaction with a hard core greatly improved the elastic $C0$ form factor. No predictions were made for magnetic scattering.

The magnetic form factors are quite sensitive to $\Delta\beta$, or the difference between the valence nucleon parameters b_i. If $\Delta\beta$ has a more fundamental origin, perhaps it comes in part from the spin-orbit splitting of the $1p$ orbitals. For example, Cammarata and Donnelly[16] managed to fit the 3.56 MeV $M1$ form factor using a Woods-Saxon potential and a $1p_{1/2}$-$1p_{3/2}$ splitting of about 3 MeV. Since these authors were concerned with the physics of the valence particles, no predictions were made for the charge form factor.

The magnitude of $\Delta\beta$ is difficult to understand solely on the basis of the $\vec{l}\cdot\vec{s}$ interaction when one considers the general p-shell configuration amplitudes. The amplitudes of the $(1p_{3/2})^2$ terms are at least 0.8 in the ground and 3.56 MeV states, so we would not expect a large difference in the effective b_i when the $1p_{1/2}$ orbital is included, unless the spin-orbit splitting is particularly large.

We now return to the α-d picture of ^{6}Li and speculate whether the n-p tensor interaction could contribute to $\Delta\beta$. Some time ago Satchler[17] showed that the n-p tensor interaction plus the central nucleon-nucleus interaction generates an effective central-plus-tensor potential between the two nuclei. The tensor potential has the form

$$U_T(\vec{R},\vec{S})=U_T(R)[(\vec{S}\cdot\hat{R})^2-\tfrac{2}{3}]\,, \tag{19}$$

where $\vec{S}$ is the deuteron spin, $\vec{R}$ is the relative position vector of the deuteron, and the caret denotes a unit vector. The radial dependence $U_T(R)$ is given in Satchler's paper in terms of an integral involving the deuteron internal S- and D-state wave functions.

Recently, Frick *et al.*[18] studied the scattering of 20 MeV polarized deuterons by ^{4}He and found that $U_T(R)$ was much stronger than expected, about twice the folding-model predictions. Their analysis indicates $U_T(R)$ has a node at $R\approx 2.4$ fm, and is attractive beyond this point.

If we assume a similar potential operates between the clusters in ^{6}Li, the ground state becomes a mixture of S and D states and the tensor contribution comes mainly through the (positive) off-diagonal S-D matrix element. Since the rms α-d separation is about 3.4 fm, the deuteron would be most strongly influenced by the attractive region of $U_T(R)$, and the tensor force would tend to align the deuteron spin along $\vec{R}$. The degree of intrinsic cluster deformation depends on the internal S-D admixture, but in any case the major axis would likewise be aligned along $\vec{R}$. The distortion introduced into our phenomenological model could be a reflection of this deformation, even though we have not explicitly included the D state.

To accommodate the $^1P_1$ state, which is part of the general shell-model wave function, it would be necessary to break with the usual α-d scheme and include a $^1P_1$-state deuteron in relative P-wave motion with the α cluster. However, no alignment would occur since the tensor force vanishes in the singlet state.

The 3.56 MeV (0^+) level contains no D state, but it does have an appreciable $^3P_0$ component in the shell-model basis. Since the matrix element of Eq. (19) is diagonal between triplet-P states and is positive, this level should also show evidence of an aligned deformation. Similar arguments can be made for the other levels.

Finally, one might expect the Coulomb repulsion between the proton and the ^{4}He core to polarize the deuteron cluster along $\vec{R}$. No doubt this happens to some extent since there is about 1 MeV difference in the valence-nucleon separation energies. However, if the polarization is large, it would tend to destroy the isospin purity of the levels in ^{6}Li, in contradiction to experiment. Note that in our model we have aligned the d cluster, not polarized it.

Whether any or all of these interactions is sufficient to explain $\Delta\beta$ can only be determined by detailed calculations. Anyway, the important point here is *not* whether the cluster model is a realistic picture of ^{6}Li, but rather that a simple model *is* capable of giving a unified account of the electromagnetic structure. There is no reason, therefore, not to expect at least as much from a more fundamental treatment such as the α-n-p model.

IV. COMPARISON OF THE ELASTIC AND INELASTIC $M1$ FORM FACTORS

The similarity of the elastic and inelastic (3.56 MeV) $M1$ form factors has already been noted. Here we will make a specific comparison by considering their ratio, and this can best be done by working with phenomenological fits to the individual form factors. The fitting procedure is described elsewhere for the 3.56 MeV transition.[7] We have performed a similar analysis on the present elastic data together with the Amsterdam results[1]; the

parameters are summarized in the Appendix. As before, the effective momentum transfers q_{eff} as defined by Eq. (10) were used. From these analyses the diffraction minima were accurately located, namely $q_{\min}=1.41\pm0.03$ fm^{-1} and 1.40 ± 0.01 fm^{-1} for the elastic and inelastic form factors, respectively.

The ratio of the phenomenological fits is represented by the solid curve in Fig. 3. (This curve does not take into account the uncertainties in the $q_{\min}$.) For convenience the ratio has been normalized to unity at $q=0$ according to the relation

$$\frac{F_{M1}^2(3.56)}{F_{M1}^2(\text{gnd})} \underset{q\to 0}{\to} \frac{\Gamma_{\gamma 0} m_p^2}{2\alpha\mu^2\omega^3}=16.12\ , \tag{20}$$

where $\Gamma_{\gamma 0}$ is the $M1$ radiative width (8.16 eV), ω is the excitation energy, and $\mu=0.822$ is the ground-state magnetic moment. Also shown in the figure are the inverse ratios of the elastic data to the inelastic fit, renormalized as above.

Two peculiar features are evident. First, the diffraction minima are nearly coincident, and second,

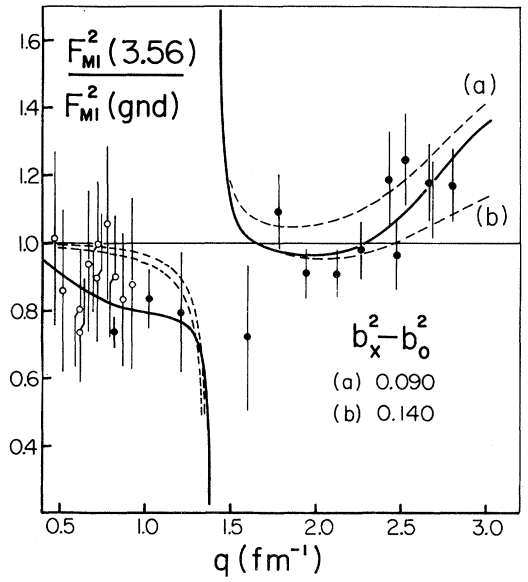

FIG. 3. Ratio of the inelastic (3.56 MeV) to elastic $M1$ form factors, normalized to unity at $q=0$. The solid line is derived from the phenomenological fits to the data. The indicated data points are derived from the present experiment (black points) and the Amsterdam work (open circles). The dashed curves represent the harmonic-oscillator models modified by MEC as discussed in the text. The unmodified minima are at $q_0=1.41$ fm^{-1} and $q_x=1.37$ fm^{-1} for the elastic and inelastic form factors, respectively, while b_0 and b_x are the corresponding oscillator parameters, in fm.

the 3.56 MeV form factor decreases more slowly at high momentum transfers than the elastic form factor. Both results are contrary to expectation as can be seen from the following argument. In a $(1p)^2$ harmonic oscillator configuration space the form factors satisfy

$$\frac{F_{M1}^2(3.56)}{F_{M1}^2(\text{gnd})}=A\left[\frac{1-\left[\frac{q}{q_x}\right]^2}{1-\left[\frac{q}{q_0}\right]^2}\right]^2 e^{(1/2)q^2(b_0^2-b_x^2)}\ , \tag{21}$$

where q_0 and q_x are the positions of the elastic and inelastic diffraction minima, and (b_0,b_x) are the corresponding effective oscillator parameters. The constant A is the relative normalization at $q=0$. Although the individual form factors are not well represented in the harmonic oscillator basis, it should suffice for describing the general features of their *ratio*. The usual proton and c.m. corrections tend to cancel in the ratio and are not included.

Now, the inelastic transition-density radius is expected to be larger than the corresponding ground state quantity in view of the difference in binding energies, and this implies $q_0>q_x$. From binding energy considerations one also expects $b_x>b_0$ which according to Eq. (21) would result in a decrease in the ratio with increasing q, contrary to experiment.

One possible explanation may lie in the various two-body processes collectively referred to as meson exchange currents (MEC). These contribute to the inelastic transition because of its isovector character but are much less effective in the ground state. Haxton and Dubach[19] have computed the effects of MEC on the 3.56 MeV form factor for a variety of harmonic oscillator wave functions, and we will refer to their results for the Donnelly-Walecka amplitudes[16] since these yield a diffraction minimum near $q=1.4$ fm^{-1}.

A measure of the MEC is given by the ratio

$$R(q)=\frac{F_{M1}^2(1+2)}{F_{M1}^2(1)}\ ,$$

where the numerator contains both one- and two-body terms, while the denominator retains only the usual one-body terms. Inspection of $R(q)$ vs q for the Haxton-Dubach calculation shows that the one- and two-body terms interfere constructively for $q<q_{\min}$ and destructively for $q>q_{\min}$; in other words the inelastic diffraction minimum is shifted to *higher* momentum transfers relative to the one-body theory. Furthermore, $R(q)$ increases uniform-

ly from $q_{\min}$ through the highest q values of our measurements.

To compare with experiment we have scaled Eq. (21) by $R(q)$, treating q_x and $(b_x{}^2-b_0{}^2)$ as variables, while $q_0=1.41$ fm^{-1} was fixed by the elastic $M1$ form factor. The normalization is unity at $q=0$, that is, $A=R^{-1}(q=0)$. The two variables were then chosen to give the best overall agreement with the experimental form factor ratio.

The results are summarized by the two dashed curves in Fig. 3 which roughly bracket the data at high momentum transfers. The minimum of the one-body inelastic form factor is now $q_x=1.37$ fm^{-1}, and $b_x>b_0$ as one would expect. Although some discrepancy exists at low momentum transfers, the general trend of the experimental ratio is reproduced. Until calculations are done with more realistic wave functions, we can only conclude that the theoretical two-body effects seem to be operating in a direction which is consistent with the experimental form factors.

V. GROUND-STATE CURRENT DENSITY

In principle, the ground-state charge and current densities can be deduced from the experimental Coulomb and magnetic form factors, providing the data span a sufficiently large range of momentum transfers. In practice, the data are limited and one either fits to a phenomenological density, or, as in the Fourier-Bessel method, one makes an assumption about the asymptotic behavior of the form factor. The latter technique, applied first to charge scattering[20] and later to inelastic magnetic transitions,[7,21] is becoming more popular as the quality and range of the electron scattering data expand. Here, we apply it to the elastic $M1$ form factor of ^{6}Li to deduce the ground-state current density.

The part of the nuclear current density which contributes to the elastic $M\lambda$ scattering from a nucleus of spin J may be written[7]

$$\vec{J}(\vec{r})=[2J+1]^{-1/2}(JM\lambda\mu\,|\,JM')J_{\lambda\lambda}(r)\vec{Y}^{\mu*}_{\lambda\lambda 1}(\Omega_r)\ , \tag{22}$$

where $J_{\lambda\lambda}(r)$ describes the radial distribution of the current, and is the quantity we wish to determine. It is related to the form factor by the expressions

$$F_{M\lambda}{}^2=\frac{4\pi}{Z^2}\frac{1}{2J+1}\,|\,\langle J||T^{\rm mag}_\lambda(q)||J\rangle\,|^2 \tag{23}$$

and

$$\langle J||T^{\rm mag}_\lambda(q)||J\rangle=\int_0^\infty j_\lambda(qr)J_{\lambda\lambda}(r)r^2dr\ . \tag{24}$$

We expand $J_{\lambda\lambda}(r)$ in a truncated Fourier-Bessel series within a region $r\le R$,

$$J_{\lambda\lambda}(r)\approx\sum_{\nu=1}^{N}a_\nu j_\lambda(q_\nu r)\ ,\quad r\le R\ ,$$
$$=0\ ,\quad r>R\ , \tag{25}$$

where $q_\nu R$ are the zeros of j_λ, that is, $j_\lambda(q_\nu R)=0$. The method for choosing N and R is somewhat subjective and is described in detail in Ref. 7. Beyond the last data point the form factor is assumed to lie, with uniform probability, within the envelope $F_{\max}=\pm A_1e^{-B_1q}$, where $A_1=0.0206$ and $B_1=0.977$ in the present case. This is a linear function on a logarithmic plot which is tangent to both lobes of the experimental form factor. Finally, the expansion coefficients a_ν are determined by a least-squares fit to the data and again we refer the reader to Ref. 7 for a more detailed explanation.

The $M1$ current density obtained from the combined Bates (present experiment) and Amsterdam[1] data is shown in Fig. 4, and the Fourier-Bessel coefficients are tabulated in Table II. The effective momentum transfers $q_{\rm eff}$ were used, and the fit was constrained at $q=0$ by the known magnetic moment of ^{6}Li.

The ground-state (isoscalar) current bears a striking resemblance to the (isovector) $M1$ transition currents of the 3.56 MeV state of ^{6}Li (Ref. 7) and the 15.11 MeV state of ^{12}C (Ref. 21), aside from overall scale factors. All have a node near

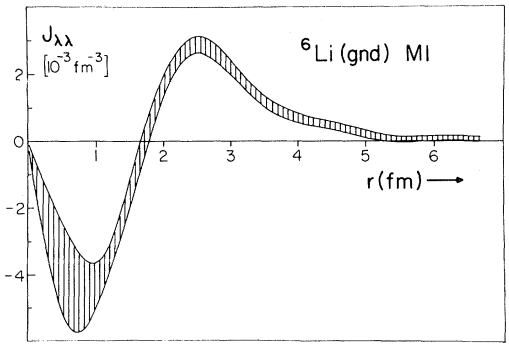

FIG. 4. The radial dependence of the ground-state current density of ^{6}Li as determined from a combination of the present and Amsterdam data. The error band represents ±1 standard deviation from the nominal density.

TABLE II. Fourier-Bessel coefficients for the ground-state $M1$ current density.

ν	$a_\nu \times 10^4$ (fm^{-3})	q_ν (fm^{-1})
1	16.17±0.31	0.5912
2	23.34±0.73	1.0165
3	−1.96±1.65	1.4348
4	−33.36±0.99	1.8508
5	−44.75±1.17	2.2659
6	−36.00±0.98	2.6804
7	−17.48	3.0947
8	5.78	3.5087
9	−2.21	3.9226
10	0.90	4.3364
11	−0.38	4.7501
$\chi_\nu^2(pdf)=0.61$		
$N_i=6$, $N-N_i=5$		
$R=7.600$ fm		

$r=1.7-1.8$ fm and exhibit a "knee" around $r=3.5$ fm. In part the similarity is due to the fact that the three form factors have minima around $q=1.4$ fm^{-1} and the convection currents play a minor role in each.

When normalized to a common scale, the 3.56 MeV transition current is slightly stronger than the ground-state current on the first extremum of $J_{\lambda\lambda}(r)$ ($r\approx 0.8$ fm) but weaker in the region $r=2.5-4.0$ fm, although the error bands do overlap to some extent. One can show that this is precisely the behavior required to produce a form factor ratio which increases at high q. If the two-body effects are indeed responsible, then they are suppressing the nuclear current near the surface while enhancing it deep within the nucleus.

Precise measurements of the $M1$ form factors at even higher momentum transfers are required if we wish to reduce the statistical overlap of the error bands to the point where the differences, if real, are clear. Anyway, from the discussion in Sec. IV, even the similarity of the current distributions is unexpected unless we invoke some device for increasing the isovector cross section at high momentum transfer.

ACKNOWLEDGMENTS

We are indebted to W. Haxton and J. Dubach for providing us with the results of their exchange-current calculations prior to publication and for conversations concerning them. L. Lapikás kindly provided us with the Amsterdam (IKO) 180° scattering data on ^{6}Li. We wish to acknowledge the invaluable assistance rendered during the experimental phase by K. Itoh, B. E. Norum, and J. Lichtenstadt. This work was supported in part through funding for the Bates Accelerator Laboratory provided by the U. S. Department of Energy under Contract No. EY-76-C-02-3069. One of us (J.C.B.) acknowledges the support of the Natural Sciences and Engineering Research Council of Canada.

APPENDIX: PHENOMENOLOGICAL ANALYSIS OF THE ELASTIC $M1$ FORM FACTOR

The analysis formalism and notation have been described in detail elsewhere[7] and will not be reviewed here. The form factor may be written

$$F_{M1}=q\,[K_0\langle j_0(qr)\rangle+K_2\langle j_2(qr)\rangle]\ ,$$

where K_0 and K_2 depend only on the configuration amplitudes (α,β,γ), defined by

$$\psi_{1^+,0}(\text{gnd})=\alpha^3S_1+\beta^1P_1+\gamma^3D_1\ .$$

As before, we use

$$\alpha=0.924\ ,\quad \beta=0.369\ ,\quad \gamma=0.102\ ,$$

which reproduce the experimental magnetic moment. They give

$$K_0=3.326\times 10^{-2}\ \text{fm}\ ,$$

$$K_2=2.803\times 10^{-3}\ \text{fm}\ .$$

The parameters (b,a_n) of the radial density

$[R(r)]^2$ were determined by a least-squares fit to the combined Bates-Amsterdam data (27 points), with the density normalized to unity. The results are as follows:

$$\chi_\nu^2(pdf)=0.68\ ,$$

$$b=2.265\ \text{fm}\ ,$$

$$a_2=9.870\times10^{-2}\ \text{fm}^{-5}\ ,$$

$$a_3=-3.854\times10^{-2}\ \text{fm}^{-6}\ ,$$

$$a_4=4.858\times10^{-3}\ \text{fm}^{-7}\ ,$$

$$a_6=-2.278\times10^{-5}\ \text{fm}^{-9}\ ,$$

$$a_8=1.533\times10^{-7}\ \text{fm}^{-11}\ .$$

The rms radius of $[R(r)]^2$ is 3.24 fm, compared with 3.46 fm for the 3.56 MeV $M1$ transition.

[1]L. Lapikás, in Proceedings of the Conference on Modern Trends in Elastic Electron Scattering, Amsterdam, 1978 (unpublished) and private communication.

[2]R. E. Rand, R. Frosch, and M. R. Yearian, Phys. Rev. 144, 859 (1966).

[3]D. R. Lehman, Mamta Rai, and A. Ghovanlou, Phys. Rev. C 17, 744 (1978) and references therein; W. C. Parke *et al.*, Phys. Lett. 74B, 158 (1978).

[4]J. C. Bergstrom, Nucl. Phys. A327, 458 (1979).

[5]W. Bertozzi, M. V. Hynes, C. P. Sargent, W. Turchinetz, and C. Williamson, Nucl. Instrum. Methods 162, 211 (1979).

[6]G. A. Peterson, J. B. Flanz, D. V. Webb, H. de Vries, and C. F. Williamson, Nucl. Instrum. Methods 160, 375 (1979).

[7]J. C. Bergstrom, U. Deutschmann, and R. Neuhausen, Nucl. Phys. A327, 439 (1979).

[8]L. C. Maximon, Rev. Mod. Phys. 41, 193 (1969).

[9]R. E. Rand, Nucl. Instrum. Methods 39, 45 (1966).

[10]H. A. Bethe and J. Ashkin, in *Experimental Nuclear Physics,* edited by E. Segrè (Wiley, New York, 1953), Vol. I.

[11]G. C. Li, I. Sick, R. R. Whitney, and M. R. Yearian, Nucl. Phys. A162, 583 (1971).

[12]Yu. A. Kudeyarov, I. V. Kurdyumov, V. G. Neudatchin, and Yu. F. Smirnov, Nucl. Phys. A163, 316 (1971).

[13]F. Ajzenberg-Selove, Nucl. Phys. A320, 1 (1979).

[14]J. C. Bergstrom, Phys. Rev. C 21, 2496 (1980).

[15]G. L. Payne and B. P. Nigam, Phys. Rev. C 21, 1177 (1980).

[16]J. B. Cammarata and T. W. Donnelly, Nucl. Phys. A267, 365 (1976).

[17]G. R. Satchler, Nucl. Phys. 21, 116 (1960).

[18]R. Frick, H. Clement, G. Graw, P. Schiemenz, and N. Seichert, Phys. Rev. Lett. 44, 14 (1980).

[19]W. Haxton and J. Dubach (unpublished).

[20]B. Dreher, J. Friedrich, K. Merle, H. Rothhaas, and G. Lührs, Nucl. Phys. A235, 219 (1974).

[21]U. Deutschmann, G. Lahm, R. Neuhausen, and J. C. Bergstrom, in Contributed Abstracts to the Proceedings of the International Conference on Nuclear Physics, Berkeley, 1980, LBL Report No. LBL-11118.